

# Mathematical Model for the Population Dynamics of *Aedes aegypti* Under Extreme Temperature Conditions

**Original Research  
Article**

---

## Abstract

**Aims/ objectives:** To develop and analyze a mathematical model for the population dynamics of *Aedes aegypti* under extreme temperature conditions, focusing on endemic and non-endemic regions of Salta, Argentina.

**Study design:** Deterministic mathematical modeling study.

**Place and Duration of Study:** Faculty of Natural Sciences and Faculty of Exact Sciences, National University of Salta, Argentina; simulations and analysis conducted during the research period 2025.

**Methodology:** Building upon the differential equation framework proposed by Yang et al., entomological parameters were redefined using piecewise continuous functions to extend validity beyond the experimental range of 10–40 °C. The model incorporates larval, pupal, and adult stages. Equilibrium points and stability were analyzed through Routh–Hurwitz criteria. Sensitivity analysis of the temperature-dependent basic offspring number  $Q_0^*(T)$  was conducted, and numerical simulations were performed for three contrasting departments (Orán, Capital, La Poma).

**Results:** The analysis shows that mosquito persistence or extinction is strongly conditioned by temperature through  $Q_0^*(T)$ . Parameters such as oviposition rate, larval survival, and the proportions of larvae and female adults ( $k$  and  $f$ ) are the most influential. Simulations reproduce local patterns: persistence in warmer regions (Orán, Capital) and extinction in colder regions (La Poma), consistent with field data.

**Conclusion:** The extended model ensures mathematical consistency under extreme temperatures and provides a consistent framework for predicting vector dynamics in diverse climatic scenarios. These findings strengthen the link between theoretical modeling and empirical evidence, offering relevant implications for public health strategies against dengue in northern Argentina.

**Keywords:** *Aedes*, dengue, temperature, modeling, stability, sensitivity.

2010 Mathematics Subject Classification: 53C25; 83C05; 57N16

---

---

# 1 Introduction

Dengue is a viral disease transmitted through the bite of the *Aedes aegypti* mosquito, which has affected the province of Salta, Argentina, for more than 20 years (National Directorate of Epidemiology and Health Situation Analysis, 2021; Avilés, 2000; Chanampa, 2019). Understanding aspects of the vector's population dynamics, based on estimates of local parameters, is of great importance.

If the disease is not controlled through mosquito eradication, more pronounced outbreaks could occur in the coming years, potentially overwhelming the resources of the provincial health system. For instance, in 2023 Argentina registered 16,143 cases of dengue up to week 12. This number represents a significant increase compared to the last two years, although it is still 10% lower than in 2020 and 40% lower than in 2016, two previous epidemic seasons (General Directorate of Epidemiological Coordination, 2023).

In this epidemiological context, it is crucial to analyze the problem from a mathematical perspective, with the aim of understanding and predicting key aspects of disease spread. Dengue can be modeled, numerically simulated, and described in regional scenarios, investigating the influence of temperature in different areas of the province on the mosquito's life cycle. Yang et al. (2009, 2011) conducted laboratory experiments and showed that at low temperatures there is no development of immature forms into adults nor an increase in oviposition; while at high temperatures, only the development of immature forms is observed. Their results are based on a temperature range between 10 °C and 40 °C. These findings coincide with references from the Ministry of Public Health of Argentina. For example, *Aedes aegypti* larvae cannot withstand temperatures below 10 °C or above 45 °C; furthermore, below 13 °C the transition to the pupal stage is interrupted.

Since it is difficult to replicate these experiments in a laboratory, the mathematical results on survival rates are adapted to understand what happens in regions of interest in Salta. The city of Marília, in the state of São Paulo, Brazil, from which these rates were experimentally derived, lies within the same geographic region as the departments of Orán, Capital, and La Poma, in the province of Salta, Argentina. All of these locations are situated in the Southern Hemisphere and share similar subtropical and tropical climatic conditions, as they are aligned along a latitude close to the Tropic of Capricorn. Considering background information on the presence or absence of *Aedes aegypti* in Salta, entomological parameters were determined for Orán, Capital, and La Poma, departments located in different ecoregions and exhibiting contrasting climatic conditions. La Poma was chosen to compare findings reported in the literature with results obtained through simulations under different modeled scenarios. This comparison allows for exploring the model's limitations in contexts unfavorable for the presence of the vector.

Orán was also included due to the abundance of data and studies on the strong presence of *Aedes aegypti*, and Capital due to its history of dengue transmission under climatic conditions different from those of Orán. In total, three departments were selected that exhibit marked contrasts in temperature, vector presence, and disease prevalence. Since the regions of interest experience average annual temperatures below 10 °C, it is necessary to extend the temperature range considered in the model. To this end, a redefinition of entomological parameters using piecewise continuous functions is proposed. Yang et al. (2011) proposed a mathematical model of differential equations that describes the mosquito population dynamics, determining equilibrium points and their local stability. However, this work did not address sensitivity or bifurcation analysis. The objective of this article is to expand the study of the model by considering a redefinition of the entomological parameters, upon which all subsequent analyses are based. In particular, the stability analysis of the equilibria, the sensitivity analysis of parameters, and numerical simulations are addressed, with results compared to fieldwork carried out in Salta.

## 2 Materials and Methods

### 2.1 Entomological Parameters and Temperature Dependence

The mathematical framework used to define the entomological parameters of the model is based on the polynomial equation proposed by Yang et al. (2009, 2011). This equation describes biological rates in units of  $\text{day}^{-1}$  as a function of temperature  $T$ .

The parameters considered and their dependence on temperature  $T$  are:

- $\phi(T)$ : *Per capita* oviposition rate.
- $\mu_l(T)$ : Larval mortality rate.
- $\pi_l(T)$ : Transition rate from larva to pupa.
- $\mu_p(T)$ : Pupal mortality rate.
- $\pi_p(T)$ : Transition rate from pupa to adult.
- $\mu_f(T)$ : Adult mosquito mortality rate.

The polynomial coefficients ( $b_n$ ) and the temperature validity ranges for each parameter are presented in Table 1.

**Table 1:** Estimated coefficients for the polynomial fitting of entomological parameters as a function of temperature  $T$  (in  $^{\circ}\text{C}$ ).

| Coefficients                  | $\phi(T)$               | $\mu_l(T)$              | $\mu_p(T)$              | $\mu_f(T)$              | $\pi_l(T)$              | $\pi_p(T)$              |
|-------------------------------|-------------------------|-------------------------|-------------------------|-------------------------|-------------------------|-------------------------|
| $b_0$                         | -5.400                  | 2.315                   | $4.256 \times 10^{-1}$  | $8.692 \times 10^{-1}$  | -1.847                  | $5.397 \times 10$       |
| $b_1$                         | 1.800                   | -4.191                  | $-3.248 \times 10^{-2}$ | $-1.590 \times 10^{-1}$ | $8.291 \times 10^{-1}$  | $-2.321 \times 10$      |
| $b_2$                         | $-2.124 \times 10^{-1}$ | $-2.735 \times 10^{-2}$ | $7.060 \times 10^{-4}$  | $1.116 \times 10^{-2}$  | $-1.457 \times 10^{-1}$ | 4.212                   |
| $b_3$                         | $1.015 \times 10^{-2}$  | $-7.538 \times 10^{-4}$ | $4.395 \times 10^{-7}$  | $-3.408 \times 10^{-4}$ | $1.304 \times 10^{-2}$  | $4.213 \times 10^{-1}$  |
| $b_4$                         | $-1.515 \times 10^{-4}$ | $7.503 \times 10^{-6}$  |                         | $3.809 \times 10^{-6}$  | $-6.461 \times 10^{-4}$ | $2.545 \times 10^{-2}$  |
| $b_5$                         |                         |                         |                         |                         | $1.796 \times 10^{-5}$  | $-9.506 \times 10^{-4}$ |
| $b_6$                         |                         |                         |                         |                         | $-2.617 \times 10^{-7}$ | $2.146 \times 10^{-5}$  |
| $b_7$                         |                         |                         |                         |                         | $1.551 \times 10^{-9}$  | $-2.681 \times 10^{-7}$ |
| $b_8$                         |                         |                         |                         |                         |                         | $1.420 \times 10^{-9}$  |
| Range $[T_{\min} - T_{\max}]$ | [11.63 - 37.20]         | [10 - 40]               | [10 - 40]               | [10 - 40]               | [11.96 - 40.55]         | [10.31 - 40.08]         |

To ensure continuity of the function and to avoid mathematical inconsistencies (such as division by zero) in subsequent simulations outside the validity ranges, each parameter is redefined using the asterisk notation (for example,  $\phi^*(T)$ ). This extension considers the image of the extreme values. Thus, the rates are redefined by the following piecewise functions, as illustrated in Figure 1:

$$\begin{aligned}
 \phi^*(T) &= \begin{cases} \phi(11.63) & \text{if } T \leq 11.63 \\ \phi(T) & \text{if } 11.63 < T < 37.20 \\ \phi(37.20) & \text{if } T \geq 37.20 \end{cases} & \mu_l^*(T) &= \begin{cases} \mu_l(10) & \text{if } T \leq 10 \\ \mu_l(T) & \text{if } 10 < T < 40 \\ \mu_l(40) & \text{if } T \geq 40 \end{cases} \\
 \mu_p^*(T) &= \begin{cases} \mu_p(10) & \text{if } T \leq 10 \\ \mu_p(T) & \text{if } 10 < T < 40 \\ \mu_p(40) & \text{if } T \geq 40 \end{cases} & \mu_f^*(T) &= \begin{cases} \mu_f(10) & \text{if } T \leq 10 \\ \mu_f(T) & \text{if } 10 < T < 40 \\ \mu_f(40) & \text{if } T \geq 40 \end{cases} \\
 \pi_l^*(T) &= \begin{cases} \pi_l(11.96) & \text{if } T \leq 11.96 \\ \pi_l(T) & \text{if } 11.96 < T < 40.55 \\ \pi_l(40.55) & \text{if } T \geq 40.55 \end{cases} & \pi_p^*(T) &= \begin{cases} \pi_p(10.31) & \text{if } T \leq 10.31 \\ \pi_p(T) & \text{if } 10.31 < T < 40.08 \\ \pi_p(40.08) & \text{if } T \geq 40.08 \end{cases}
 \end{aligned} \tag{2.1}$$

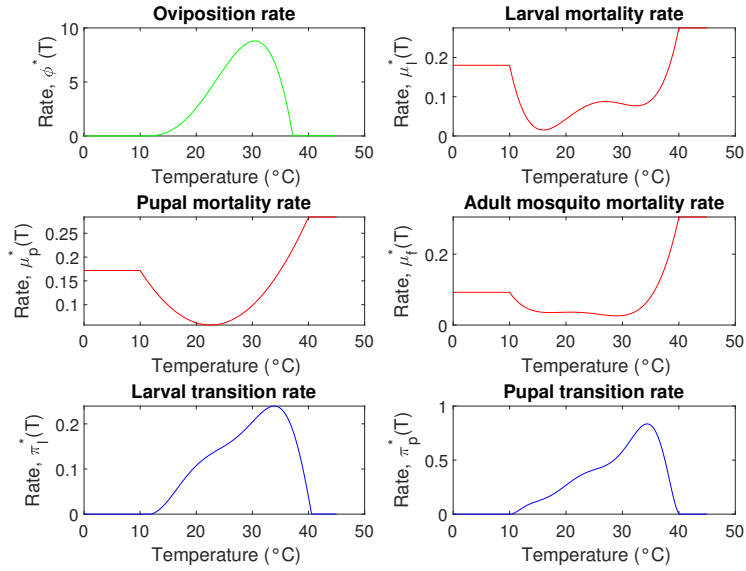


Figure 1: Entomological parameters  $\phi^*$ ,  $\mu_l^*$ ,  $\mu_p^*$ ,  $\mu_f^*$ ,  $\pi_l^*$  and  $\pi_p^*$  as a function of temperature in degrees Celsius, for  $T \in [0, 45]$ .

## 2.2 Population Dynamics Model

The population dynamics of *Aedes aegypti* are modeled based on its life cycle, composed of three stages: two aquatic phases (larva  $L$  and pupa  $P$ ) and one adult phase (mosquitoes  $M$ ) (Yang et al., 2011).

The model incorporates essential assumptions for population dynamics, such as the sufficient availability of males for mating (Eiman et al., 2010). In addition, it includes three input parameters whose values will be defined in the simulation section:

- The carrying capacity ( $C$ ) of breeding sites, understood as a standardized reproduction site (Otero et al., 2006).
- The proportion of eggs that develop into larvae ( $k$ ).
- The proportion of pupae that develop into adult females ( $f$ ).

The autonomous dynamical system is described by three nonlinear ordinary differential equations:

$$\begin{cases} \frac{dL}{dt} = kf\phi^*(T)M \left(1 - \frac{L}{C}\right) - (\pi_l^*(T) + \mu_l^*(T))L \\ \frac{dP}{dt} = \pi_l^*(T)L - (\pi_p^*(T) + \mu_p^*(T))P \\ \frac{dM}{dt} = \pi_p^*(T)P - \mu_f^*(T)M \\ L(t_0) = a, P(t_0) = b, M(t_0) = c \end{cases} \quad (2.2)$$

where all parameters are strictly positive. Based on the previous definitions and descriptions, the resulting diagram of the model is presented in Figure 2.

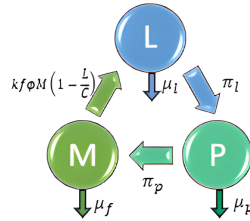


Figure 2: Flow diagram representing the population dynamics of mosquitoes

### 2.3 Equilibrium and Stability Analysis

#### 2.3.1 Biological Domain

**Theorem 2.1.** The model (2.2) is biologically and mathematically well-posed in the domain  $\Omega$ , which is positively forward invariant:

$$\Omega = \left\{ (L, P, M) \in \mathbb{R}_+^3 \mid 0 \leq L \leq C, 0 \leq P \leq \frac{\pi_l^*(T)}{\pi_p^*(T) + \mu_p^*(T)} \cdot C, 0 \leq M \leq \frac{\pi_p^*(T)}{\mu_f^*(T)} \frac{\pi_l^*(T)}{\pi_p^*(T) + \mu_p^*(T)} \cdot C \right\}$$

*Proof.* For the system of differential equations (2.2) there exists a unique solution, since the right-hand side is continuous and has continuous partial derivatives in the domain  $\Omega$ . It is shown that  $\Omega$  is positively forward invariant. The verification is carried out by analyzing the initial conditions on each boundary of the domain and evaluating the sign of the corresponding derivatives. In all cases, the flow vectors point inward or are null at the boundary, ensuring that no trajectory can leave  $\Omega$ . Therefore, any solution of system (2.2) with initial conditions in  $\Omega$  remains in  $\Omega$  for all  $t \geq 0$ .  $\square$

#### 2.3.2 Equilibrium Points

System (2.2) admits two equilibrium points: the trivial point, representing the absence of mosquitoes,

$$P_0 = (\bar{L}_0, \bar{P}_0, \bar{M}_0) = (0, 0, 0) \tag{2.3}$$

and the non-trivial point  $P_1$ , representing the presence of mosquitoes conditioned by the specific annual mean temperature  $T$ :

$$P_1 = \begin{cases} \bar{L}_1(t) = C \left( 1 - \frac{1}{Q_0^*(T)} \right) \\ \bar{P}_1(t) = \frac{\pi_l^*(T)}{\pi_p^*(T) + \mu_p^*(T)} \bar{L} \\ \bar{M}_1(t) = \frac{\pi_p^*(T)}{\mu_f^*(T)} \bar{P} \end{cases} \tag{2.4}$$

The key parameter for the existence of  $P_1$  is the Temperature-Dependent Basic Offspring Number,  $Q_0^*(T)$ , which represents the average number of viable females produced by a female throughout her lifetime, and is given by:

$$Q_0^*(T) = \frac{\pi_l^*(T)}{\pi_l^*(T) + \mu_l^*(T)} \cdot \frac{\pi_p^*(T)}{\pi_p^*(T) + \mu_p^*(T)} \cdot \frac{kf\phi^*(T)}{\mu_f^*(T)} \quad \text{with } k, f \in (0, 1) \tag{2.5}$$

### 2.3.3 Local Stability

The local stability analysis of the equilibrium points of system (2.2) is performed by evaluating the Jacobian matrix at each equilibrium state and applying the Routh-Hurwitz criterion.

**Theorem 2.2.** *Let  $Q_0^*(T)$  be a given parameter. The following local stability conditions hold:*

1. *If  $Q_0^*(T) < 1$ , the trivial equilibrium point is locally asymptotically stable.*
2. *If  $Q_0^*(T) > 1$ , the trivial equilibrium point is unstable.*
3. *If  $Q_0^*(T) > 1$ , the non-trivial equilibrium point is locally asymptotically stable.*
4. *If  $Q_0^*(T) < 1$ , the non-trivial equilibrium point is unstable.*

**Outline of the proof.** The Jacobian matrix of the system is constructed in terms of the transition and mortality rates of each stage. When evaluated at the trivial and non-trivial equilibrium points, a cubic characteristic polynomial is obtained whose coefficients depend on  $Q_0^*(T)$ . By applying the Routh-Hurwitz criterion, the sign of the real parts of the eigenvalues is determined, which allows establishing the stability conditions as a function of  $Q_0^*(T)$ .

## 3 Results and Discussion

### 3.1 Sensitivity Analysis of $Q_0^*(T)$

The behavior of the mosquito population is intrinsically linked to the value of  $Q_0^*(T)$ , as established in Theorem 2.2. Therefore, a sensitivity analysis for  $Q_0^*(T)$  is performed using the method of normalized local sensitivity coefficients. This method consists of calculating the sensitivity index  $\Gamma$  of each parameter  $p$  as:

$$\Gamma_p^{Q_0^*(T)} = \frac{\partial Q_0^*(T)}{\partial p} \frac{p}{Q_0^*(T)} \quad (3.1)$$

An analysis of the partial derivatives of  $Q_0^*(T)$  indicates that it is an increasing function of the parameters  $\phi^*(T)$ ,  $\pi_l^*(T)$ ,  $\pi_p^*(T)$ ,  $k$ , and  $f$ . Conversely,  $Q_0^*(T)$  is a decreasing function of the parameters  $\mu_l^*(T)$ ,  $\mu_p^*(T)$ , and  $\mu_f^*(T)$ .

The results of the sensitivity index calculations for  $Q_0^*(T)$  are presented in Table 2.

According to the magnitude of the indices, the most influential parameters in model (2.2) are  $\phi^*(T)$ ,  $\mu_f^*(T)$ ,  $k$ , and  $f$ , all with a magnitude of  $|1|$ . These have a significant impact on the stability of the system, whereas the parameters associated with immature stages ( $\mu_l^*(T)$ ,  $\pi_l^*(T)$ ,  $\mu_p^*(T)$ , and  $\pi_p^*(T)$ ) exhibit magnitudes lower than  $|1|$ .

Parameters  $k$ ,  $f$ , and  $\phi^*(T)$  show a directly proportional change with respect to  $Q_0^*(T)$ . For example, if  $k$  increases (or decreases) by 30%,  $Q_0^*(T)$  also varies by 30%. In contrast,  $\mu_f^*(T)$  generates an inversely proportional change in  $Q_0^*(T)$ .

### 3.2 Influence of $k$ and $f$ and Simulation Parameters

Keeping  $k$  and  $f$  constant,  $Q_0^*(T)$  follows an increasing curve in the interval  $[-15, T_{\max}]$  and a decreasing curve in  $[T_{\max}, 45]$ , with  $T_{\max} \approx 29^\circ\text{C}$ . The maximum value,  $Q_{0\max}^*$ , depends on the value of  $k$  (Figure 3a) or the value of  $f$  (Figure 3b).

Numerical experimentation with the parameters  $k$  and  $f$ , which are independent of temperature, for different values between 0 and 1, allows the following inferences:

- If  $k \rightarrow 1$ , then  $Q_{0\max}^* \rightarrow 119$  with  $f = 0.6$  (Figure 3a).
- If  $k \rightarrow 0$ , then  $Q_{0\max}^* \rightarrow 0$  with  $f = 0.6$  (Figure 3a).

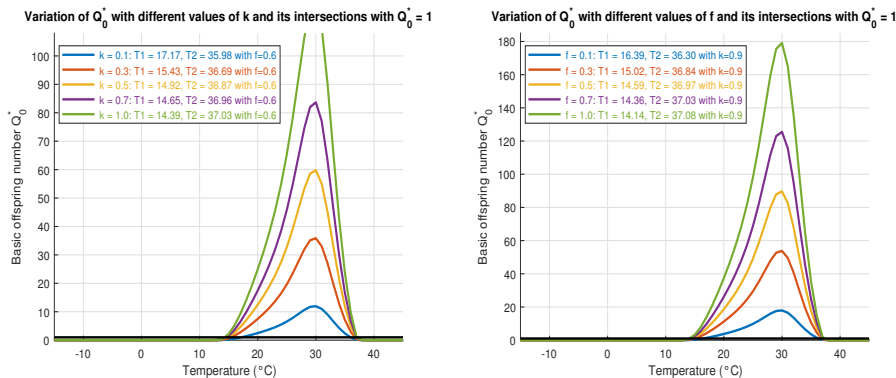
Table 2: Normalized sensitivity indices for  $Q_0^*$ .

| Parameter    | Description                                 | Index ( $\Gamma$ )   |
|--------------|---|--|
| $\phi^*(T)$  | Per capita oviposition rate at $T$          | $\Gamma_{\phi^*(T)}^{Q_0^*(T)} = 1$  |
| $\mu_l^*(T)$ | Larval mortality rate at $T$                | $\Gamma_{\mu_l^*(T)}^{Q_0^*(T)} = -\frac{\mu_l^*(T)}{\pi_l^*(T) + \mu_l^*(T)} \in (-1, 0)$ |
| $\pi_l^*(T)$ | Transition rate from larva to pupa at $T$   | $\Gamma_{\pi_l^*(T)}^{Q_0^*(T)} = \frac{\mu_l^*(T)}{\pi_l^*(T) + \mu_l^*(T)} \in (0, 1)$   |
| $\mu_p^*(T)$ | Pupal mortality rate at $T$                 | $\Gamma_{\mu_p^*(T)}^{Q_0^*(T)} = -\frac{\mu_p^*(T)}{\pi_p^*(T) + \mu_p^*(T)} \in (-1, 0)$ |
| $\pi_p^*(T)$ | Transition rate from pupa to adult at $T$   | $\Gamma_{\pi_p^*(T)}^{Q_0^*(T)} = \frac{\mu_p^*(T)}{\pi_p^*(T) + \mu_p^*(T)} \in (0, 1)$   |
| $\mu_f^*(T)$ | Adult mosquito mortality rate at $T$        | $\Gamma_{\mu_f^*(T)}^{Q_0^*(T)} = -1$  |
| $k$          | Proportion of eggs that develop into larvae | $\Gamma_k^{Q_0^*(T)} = 1$  |
| $f$          | Proportion of adult females                 | $\Gamma_f^{Q_0^*(T)} = 1$  |

- If  $f \rightarrow 1$ , then  $Q_{0 \max}^* \rightarrow 179$  with  $k = 0.9$  (Figure 3b).
- If  $f \rightarrow 0$ , then  $Q_{0 \max}^* \rightarrow 0$  with  $k = 0.9$  (Figure 3b).

The results indicate that the parameters  $k$  and  $f$  can induce extremely high or low values of  $Q_0^*$ , regardless of temperature, which in certain scenarios may be biologically unrepresentative. On the other hand, Figures 3a and 3b show that, when varying the values of  $k$  and  $f$ , the temperatures at which the threshold  $Q_0^*(T) = 1$  is crossed are close to each other and lie approximately within the interval  $[14^\circ\text{C}, 37^\circ\text{C}]$ . In this range,  $Q_0^*(T) > 1$ , and therefore the non-trivial equilibrium  $P_1$  becomes asymptotically stable. Conversely, for temperatures below  $14^\circ\text{C}$  and above  $37^\circ\text{C}$  (i.e., within the intervals  $[-15^\circ\text{C}, 14^\circ\text{C}]$  and  $(37^\circ\text{C}, 45^\circ\text{C}]$ ), it holds that  $Q_0^*(T) < 1$ , and the trivial equilibrium  $P_0$  becomes asymptotically stable.

This behavior, as evidenced in the figures, shows that the persistence of the vector's biological cycle critically depends on the fraction of larvae reaching adulthood ( $k$ ) and the proportion of eggs developing into females ( $f$ ). Both parameters determine the threshold-crossing temperatures of  $Q_0^*(T) = 1$ , and therefore condition the stability of the equilibria  $P_0$  and  $P_1$  as a function of temperature.



(a) Influence of  $k$  on  $Q_0^*(T)$  for  $0 < k < 1$  (b) Influence of  $f$  on  $Q_0^*(T)$  for  $0 < f < 1$

Figure 3: Influence of  $k$  or  $f$  on  $Q_0^*(T)$  for  $T \in [-15, 45]$

For this study, favorable probabilities for mosquito population growth are assumed, fixing the temperature-independent parameters at  $k = 0.9$  and  $f = 0.6$ . This choice is justified as follows:

- Parameter  $k$ : In departments with tropical or subtropical climates (Salta), it is reasonable to assume that nearly all *Aedes aegypti* eggs hatch ( $k = 0.9$ ), consistent with Arias et al. (2018), although it is acknowledged that for regions such as La Poma this value should be lower. It is kept fixed for comparison with other models.
- Parameter  $f$ : The value  $f = 0.6$  is used as a baseline, similar to that proposed by Arias et al. (2018). Values of  $f$  close to zero imply that no female individuals are produced, which means that the offspring number would be null for any temperature. This situation prevents the analysis of population variation, since the life cycle is canceled from the outset.

Regarding parameter  $C$ , model (2.2) uses it as the carrying capacity, representing the maximum number of individuals that an environment can support, which indeed influences the magnitude of equilibrium populations.

However, the value of  $C$  does not alter  $Q_0^*$ ; consequently, it does not affect the stability of model (2.2). As in Arias et al. (2015), the value of  $C$  is normalized to 1. This is not a real biological value or an empirical estimate, but rather a standardization for the analysis of model (2.2), which is maintained throughout the study in order to compare results at different mean temperatures across departments of Salta, Argentina.

### 3.3 Numerical Simulation and Population Dynamics

The numerical solution of system (2.2) was obtained using the *ode45* function in MATLAB, which implements a fourth–fifth order Runge–Kutta method with adaptive time step. Initial conditions  $L(t_0)$ ,  $P(t_0)$ ,  $M(t_0)$  with  $t_0 = 0$  were considered, belonging to the domain  $\Omega$ , which is positively invariant. The simulation time was set to one year, assigning the following annual mean temperatures  $T$ : 22 °C for Orán, 16 °C for Capital, and 6.5 °C for La Poma, corresponding to different departments of the province of Salta.

The values of  $Q_0^*(T)$  and the behavior of the solutions for three representative departments (Orán, Capital, La Poma) confirm the prediction of the stability analysis in Theorem 2.2:

- When  $Q_0^*(T) > 1$  (Orán and Capital), the solution converges to the non-trivial equilibrium state ( $P_1$ ) as  $t \rightarrow \infty$ , indicating processes of (re)colonization (see Figures 4a and 4b).
- When  $Q_0^*(T) < 1$  (La Poma), the solution converges to the trivial equilibrium state ( $P_0$ ), reflecting the long-term absence of mosquitoes (see Figure 4c).

Chanampa et al. (2019), based on their field results, reported the presence of *Aedes aegypti* in different localities of the province of Salta, with greater abundance in warmer areas such as Orán and lower abundance in colder regions such as La Poma. In contrast, the mathematical model predicts vector persistence only when  $Q_0^*(T) > 1$ , which corresponds to the stable non-trivial equilibrium. Thus, the observed presence in Orán is interpreted as empirical evidence consistent with the theoretical persistence predicted by the model, while the absence in La Poma reflects the extinction predicted by the trivial equilibrium ( $Q_0^*(T) < 1$ ). This distinction allows linking field data with mathematical predictions, reinforcing the validity of the approach.

Abán et al. (2022) noted that the study focuses on Orán as an area where field data confirm that the mosquito *Aedes aegypti* maintains an active, widespread, and persistent presence in the city. In this sense, the larger magnitude of  $Q_0^*(T)$  in Orán (34.148), compared to Capital (4.6774), reflects a significantly higher level of population persistence at the non-trivial equilibrium, as shown in Figures 4a and 4b, in agreement with empirical evidence. Thus, the elevated value of  $Q_0^*(T)$  in Orán is consistent with the sustained presence of *Aedes aegypti* reported by Abán et al., while Chanampa et al. indicate that in Capital the presence of the vector is lower, which corresponds to the reduced value of  $Q_0^*(T)$ . Unlike Yang et al. (2009, 2011), who fitted entomological parameters using polynomials in the range

10°C – 40°C, and Otero et al. (2006), who employed the Schoolfield equation to describe functional dependence on temperature, this work proposes a piecewise redefinition of the parameters. This strategy ensures mathematical continuity and avoids inconsistencies outside experimental intervals, allowing the analysis to be extended to extreme temperature scenarios such as those observed in La Poma. In this way, the validity of equilibrium and stability conclusions is preserved, and the applicability of the model in local contexts is reinforced.

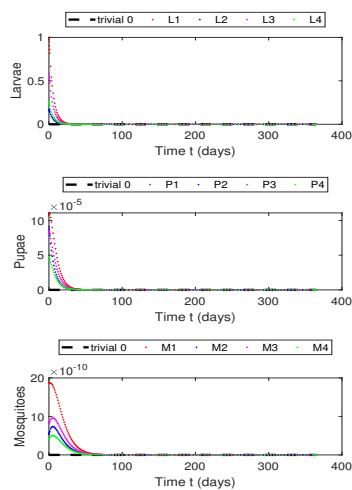
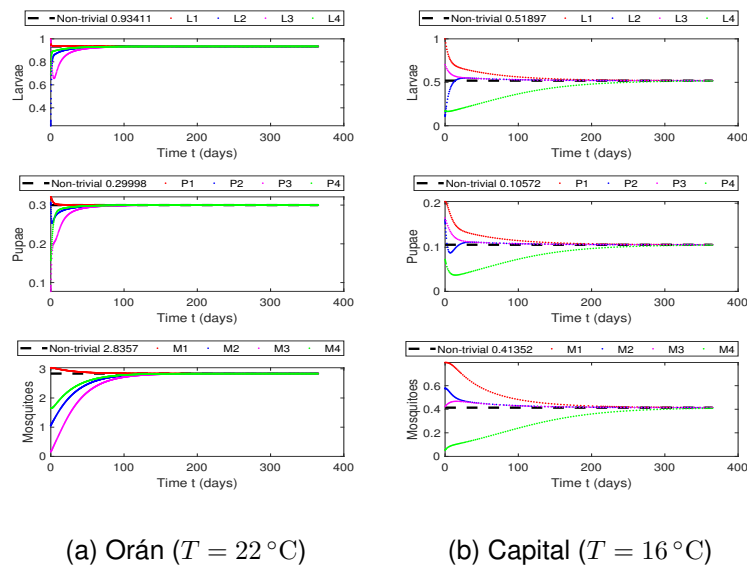


Figure 4: Numerical simulations of the population dynamics of *Aedes aegypti* in three departments of Salta.

### 3.4 Bifurcation

The stability is summarized in Figure 5, where the vertical axis represents the first component of the equilibrium points and the horizontal axis corresponds to the bifurcation parameter  $Q_0^*(T)$ . For the construction of the curve  $\bar{L}_0$ , Equation (2.3) is employed, while for the curve  $\bar{L}_1$ , Equation (2.4) is used, considering  $Q_0^*(T)$  as the variable and keeping  $k$ ,  $f$ , and  $C$  constant.

The equilibrium  $\bar{L}_1$  always exists mathematically, since by definition  $Q_0^*(T)$  is positive; however, it is biologically valid only if  $Q_0^*(T) > 1$ . Thus, when  $Q_0^*(T) < 1$ , the trivial equilibrium  $\bar{L}_0$  is asymptotically stable; whereas, once the threshold  $Q_0^* = 1$  is crossed,  $\bar{L}_1$  becomes asymptotically stable and  $\bar{L}_0$  loses stability.

Consequently, the bifurcation is transcritical: at the critical point the equilibria persist but exchange stability.

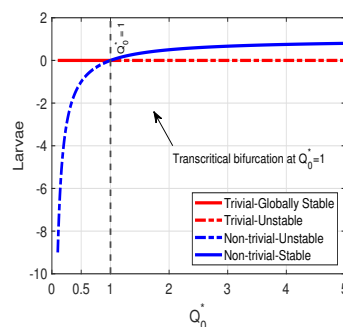


Figure 5: Bifurcation Diagram

## 4 CONCLUSIONS

- a In Section (1), the epidemiological context and the dengue problem in the province of Salta were presented, highlighting the relevance of a mathematical approach for its study. Existing knowledge and previous mathematical models related to dengue transmission and the dynamics of its vector, *A. aegypti*, were reviewed. Based on this introduction, the objectives guiding the present research were formally established, together with the working hypothesis.
- b In Section (2), the population model of *Aedes aegypti*, along with its equilibrium points and stability conditions, was originally proposed by Yang et al. for entomological parameters defined in the range of 10 to 40°C. In this work, that temperature range was extended through a piecewise redefinition of the entomological parameters, ensuring mathematical continuity and consistency. It was verified that the equilibrium and stability conclusions obtained by Yang remain valid under this extension, and it was additionally demonstrated that the biological domain, now explicitly conditioned by temperature, is positively invariant. In summary, with this modification in the definition of entomological parameters, the system preserves its mathematical and ecological validity.
- c In Section (3), the analysis confirms that the population dynamics of *Aedes aegypti* are strongly conditioned by temperature through  $Q_0^*(T)$ , with the parameters  $\phi^*(T)$ ,  $k$ ,  $f$ , and  $\mu_f^*(T)$  being the most determinant. The simulations show that the model reproduces local patterns of persistence in warmer regions (Orán, Capital) and extinction in colder regions (La Poma), thereby verifying the theoretical predictions and ensuring the biological coherence of the approach. Furthermore, the presence of a *transcritical bifurcation* is observed at the threshold

---

$Q_0^*(T) = 1$ , where stability shifts from the trivial equilibrium ( $P_0$ ) to the non-trivial equilibrium ( $P_1$ ). This result confirms that the persistence or extinction of the vector depends critically on the annual mean temperature, reinforcing the biological interpretation of the model.

## References

1. Dirección Nacional de Epidemiología y Análisis de Situación de Salud. (2021). Ministerio de Salud de la Nación: Boletín Integrado de Vigilancia, (296, 335, 447, 479, 410, 613, 561).
2. Avilés, G., Rangeon, G., Baroni, P., Paz, V., Monteros, M., Enria, D., & Sartini, J. L. (2000). Epidemia por virus dengue-2 en Salta, Argentina, 1998.
3. Chanampa, M. M., Gleiser, R., & Aparicio, J. P. (2019). Distribución y abundancia de *Aedes aegypti* en la provincia de Salta: asociación con factores ambientales.
4. Dirección General de Coordinación Epidemiológica. (2023). Boletín Epidemiológico - Provincia de Salta, Argentina. [http://saladesituacion.salta.gov.ar/web/inicio/boletines/documentos/boletin\\_132023.pdf](http://saladesituacion.salta.gov.ar/web/inicio/boletines/documentos/boletin_132023.pdf)
5. Yang, H. M., Macoris, M. L. D. G., Galvani, K. C., Andrighetti, M. T. M., & Wanderley, D. M. V. (2009). Assessing the effects of temperature on the population of *Aedes aegypti*, the vector of dengue. *Epidemiology and Infection*, 137(8), 1188–1202. <https://doi.org/10.1017/S0950268808001907>
6. Yang, H. M., Boldrini, J. L., Fassoni, A. C., Freitas, L. F., Gomez, M. C., de Lima, K. K., & de Oliveira, F. T. M. (2011). *Aedes aegypti* population dynamics: Model comparison. *Ecological Modelling*, 222(19), 3601–3611. <https://doi.org/10.1016/j.ecolmodel.2011.07.013>
7. Eiman, M., et al. (2010). Directrices para el control de vectores. Organización Mundial de la Salud.
8. Otero, M., Solari, H. G., & Schweigmann, N. (2006). A stochastic population dynamics model for *Aedes aegypti*: Mathematical analysis and validation. *Ecological Modelling*, 198(3–4), 316–332. <https://doi.org/10.1016/j.ecolmodel.2006.05.011>
9. Arias, J. H., Martínez, H. J., Sepúlveda, L. S., & Vasilieva, O. (2018). Estimación de los parámetros de dos modelos para la dinámica del dengue y su vector en Cali, Colombia. *Ingeniería y Ciencia*, 14(28), 69–92.
10. Arias, J. H., Martínez, H. J., Sepulveda, L. S., & Vasilieva, O. (2015). Predator-prey model for analysis of *Aedes aegypti* population dynamics in Cali, Colombia. *International Journal of Pure and Applied Mathematics*, 105(4), 561–597.
11. Abán Moreyra, D. N., Castillo, P. M., Escalada, A., Mangudo, C., Copa, G. N., Gleiser, R. M., Nasser, J. R., & Gil, J. F. (2022). Use of *Aedes aegypti* oviposition surveillance and a geographic information system for planning antivectorial measures. *The American Journal of Tropical Medicine and Hygiene*, 107(4), 916–924. <https://doi.org/10.4269/ajtmh.21-0364>